6

Stomata

The evolution of the stomatal apparatus was one of the most important steps in the early colonisation of the terrestrial environment. Even though the stomatal pores when fully open occupy between about 0.5 and 5% of the leaf surface, almost all the water transpired by plants, as well as the CO_2 absorbed in photosynthesis, passes through these pores. It is only in rare cases such as in the fern ally, *Stylites* from the Peruvian Andes, that CO_2 may be absorbed through the roots (Keeley *et al.* 1984). The central role of the stomata in regulating water vapour and CO_2 exchange by plant leaves is illustrated in Fig. 6.1. This figure also shows some of the complex feedback and feedforward control loops that are involved in the control of stomatal aperture and hence of diffusive conductance. It is the extreme sensitivity of the stomata to both environmental and internal physiological factors that enables them to operate in a manner that optimises the balance between water loss and CO_2 uptake.

This chapter outlines the fundamental aspects of stomatal physiology, their occurrence in plants, morphology, response to environmental factors and mechanics of operation, including a description of the various control loops illustrated in Fig. 6.1. The role of the stomata in the control of photosynthesis and of water loss is discussed in more detail in Chapters 7 and 10.

Further information on stomata, their responses and mechanism of operation, may be found in texts by Jarvis & Mansfield (1981), Willmer (1983), Zeiger *et al.* (1987) and Weyers & Meidner (1990), and in the review by Cowan (1977).

Distribution of stomata

True stomata are distinguished from other epidermal pores such as hydathodes, lenticels and the pores in the thalli of some liverworts by their marked capacity for opening and closing movements. These changes in aperture depend on alterations in the size and shape of specialised

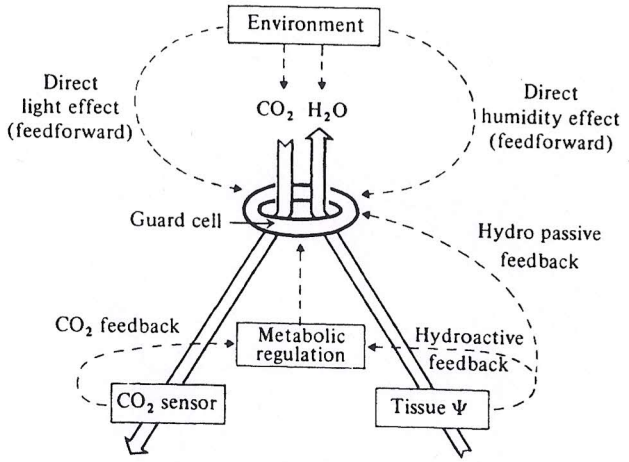

Fig. 6.1. Simplified diagram illustrating the role of stomata in regulating CO_2 and H_2O fluxes, showing the feedback and feedforward control pathways (dashed lines). For details see text. (Modified after Raschke 1975).

epidermal cells, the guard cells (Fig. 6.2). Stomata are present in the aerial parts of practically all the land flora, being found in the sporophytes of mosses, in ferns and in both gymnosperms and angiosperms. Although they are most frequent on leaves, they also occur in other green tissues such as stems, fruits and parts of inflorescences (e.g. awns of grasses and sepals of angiosperms). They tend to be most frequent on the lower surface of plant leaves, while in some species, especially trees, they occur only on the lower epidermis. Leaves with stomata on both sides are called amphistomatous, and those with stomata restricted to the lower epidermis are hypostomatous.

The two main types of stomata found in higher plants (Fig. 6.2) are (*a*) the elliptical type and (*b*) the graminaceous type, which is found in the Gramineae and Cyperaceae and has distinctive dumbbell-shaped guard cells arranged in rows. In many species, the stomata have ante-chambers outside the pore or special protective structures such as outer lips or even membrane 'chimneys' (see Fig. 6.2*d–h*), or else they are partially occluded by wax. All these features increase the effective diffusive resistance of the pore.

Representative examples of dimensions and frequencies of stomata in different species and on different leaves are presented in Table 6.1. It is clear that frequency and size vary as a function of leaf position and growth conditions. Even within one species there may be a large genetic component of the variation between different cultivars or ecotypes.

Table 6.1. *Examples showing the range of values for stomatal frequency* (ν, mm^{-2}) *and pore length* (ℓ, μm) *for different species, leaf position and growing conditions* (*–no data*)

	Adaxial surface		Abaxial surface		
	ν	ℓ	ν	ℓ	Ref.
Trees:					
Carpinus betulus	0	—	170	13	1
Malus pumila (cv. Cox)	0	—	390	21	2
Malus pumila – variation during season	0	—	230–430	—	2
Malus pumila – variation within leaf	0	—	170–360	—	2
Malus pumila – different cultivars	0	—	350–600	—	3
Pinus sylvestris	120	20	120	20	1
Picea pungens	39	12	39	12	1
Other dicots:					
Beta vulgaris	111	14.6	131	15.3	4
Tomato – low–high light	2–28	—	83–105	—	5
Soybean – range for 43 cultivars	81–174	21–23	242–385	19.5–21.7	6
Soybean – well-watered–stressed	149–158	—	357–418	—	6
Ricinus communis	182	12	270	24	1
Tradescantia virginiana	7	49	23	52	1
Grasses:					
Sorghum bicolor – mean of 6 cultivars	—	22.6	135	23	7
Hordeum vulgare – flag leaf	54–98	17–24	60–89	17	1, 8, 9
Hordeum vulgare – 5th leaf below flag	—	—	27–42	—	9

References: 1. Meidner & Mansfield 1968; 2. Slack 1974; 3. Beakbane & Mujamder 1975; 4. Brown & Rosenberg 1970; 5. Gay & Hurd 1975; 6. Ciha & Brun 1975; 7. Liang *et al.* 1975; 8. Miskin & Rasmusson 1970; 9. Jones 1977*b*.

Stomatal mechanics

Stomatal movements depend on changes in turgor pressure inside the guard cells and in the adjacent epidermal cells (which are sometimes modified to form distinct subsidiary cells). The changes in turgor can result either from

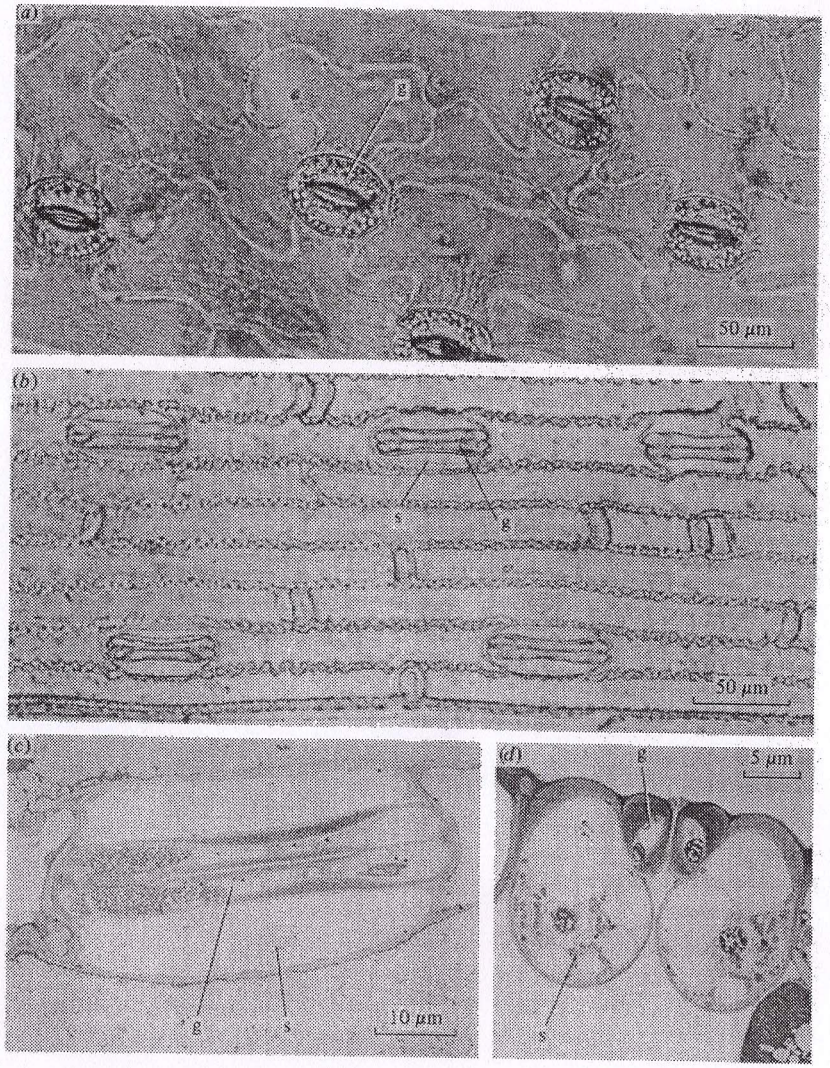

Fig. 6.2(*a*)–(*d*). For legend see opposite.

a change in total water potential (Ψ) of the guard cells as the supply or loss of water changes, or from active changes in osmotic potential (Ψ_π). The former mechanism, relying on changes *outside* the guard cells has been termed 'hydropassive' (Stålfelt 1955), while the latter has been termed 'hydroactive'. Both involve movement of water into or out of the guard cells.

Changes in guard cell turgor cause alteration in pore aperture as a

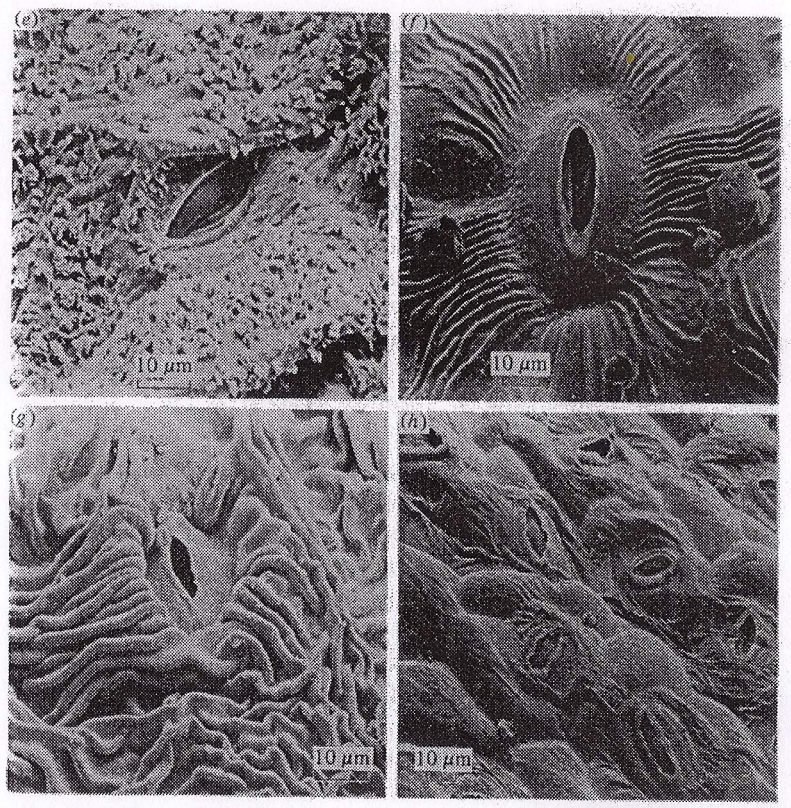

Fig. 6.2. Representative stomata from the leaves of different species: (*a*) elliptical type (abaxial surface of *Gloriosa superba*); (*b*) graminaceous type (abaxial surface of wheat, *Triticum aestivum*) (light micrographs of stripped epidermis by M. Brookfield); (*c*) and (*d*) paradermal and transverse sections, respectively, of wheat stomata showing the thickened guard cells (g) and the subsidiary cells (s) (courtesy of Dr M. L. Parker, Plant Breeding Institute, Cambridge). (*e*) to (*h*) Scanning electron micrographs of lower epidermes of some arid zone species (courtesy of Dr B. M. Joshi, University of Jodhpur) showing surface structure: (*e*) *Acacia senegal* (note the wax platelets); (*f*) *Echinops echinatus*; (*g*) *Tribulus terrestris*; (*h*) *Chorchorus tridens*.

consequence of the specialised structure and geometry of the stomatal complex. Two significant features of the commonest types of stomata are the presence of inelastic radially oriented micellae in the cell walls and a markedly thickened ventral wall (adjacent to the pore). Although it appears that neither of these characters is essential to the operation of elliptical stomata, they do influence the details of their movement (see Sharpe *et al.* 1987 for a detailed analysis of stomatal mechanics). At least for elliptical

stomata, movement probably involves deformation of the guard cells out of the plane of the epidermis, though some bulging into the subsidiary cells may also occur. The changes in guard cell volume that occur during opening are not well documented but, at least in *Vicia faba*, anatomical studies indicate that the lumen volume may double when opening from closed to an aperture of 18 μm (Raschke 1975). Stomatal apertures are approximately linearly related both to guard cell volume and, more approximately, to guard cell turgor pressure.

An important feature of stomatal operation is the role of the subsidiary cells. Analysis of stomatal mechanics has shown that in many cases the subsidiary cells have a mechanical advantage over the guard cells, such that equal increases in pressure in guard and subsidiary cells cause some closure. This implies that closure cannot normally occur as a simple hydraulic response to declining bulk leaf water status, and that all stomatal movements normally result from an active process. This conclusion is supported by the well-known observation of transient stomatal opening on excising leaves (Iwanoff 1928), which could partly be explained in terms of this mechanical advantage as bulk leaf turgor falls. The antagonism between guard and subsidiary cells has been recognised for over a century (e.g. von Mohl 1856).

Stomatal guard cells generally contain chloroplasts, though they are commonly less frequent, smaller and of different morphology to those in mesophyll cells. In spite of this widespread occurrence of chloroplasts in guard cells, however, there is little evidence that photosynthetic carbon reduction occurs or is involved in stomatal opening. Nevertheless it is likely that photophosphorylation and $NADP^+$ reduction provide energy for stomatal opening. Certain orchids (*Paphiopedilum* spp.) are exceptional in that their guard cells lack chlorophyll yet their stomata are functional (at least in intact leaves).

As we have seen, most stomatal movements, including those in response to changes in water status, involve active changes in guard cell osmotic potential. A general feature of active stomatal opening movements is that a large proportion of the osmotic material consists of potassium ions. In *Vicia faba*, for example, the K content increases from about 0.3 to 2.4 pmol per guard cell (90×10^{-6} to 680×10^{-6} mol m^{-3}) as stomata open (MacRobbie 1987). It is now generally accepted that this K^+ uptake is driven by ATP-powered primary proton extrusion at the plasmalemma. This sets up an electrical driving force for cation entry and a pH gradient (cytoplasm alkaline). The pH gradient may be dissipated by synthesis of malic acid in the cytoplasm or by chloride uptake by co-transport with protons. The malate is generated within the guard cells from storage carbohydrates such as starch, though in *Allium* species (which lack starch in their guard cells), Cl^- provides the counterion for K^+.

It has been estimated for *Vicia faba* (Allaway 1973; Allaway & Hsiao 1973) that an increase in pore width of 10 μm requires a 1.25 MPa decrease in osmotic potential, which can be largely accounted for by the increase in potassium malate. The well-known decrease in starch content that occurs in the guard cells of many species as stomata open may provide both organic anions and energy for the ion pumps. Stomatal closure is also usually an active metabolic process and does not just rely on ion leakage.

There is now strong circumstantial evidence that the plant growth regulator abscisic acid (ABA) is involved in regulating stomatal responses, especially those involving water stress. For example, externally applied ABA closes stomata, levels of endogenous ABA increase rapidly in stress (often in parallel to stomatal closure), and mutants that are deficient in the capacity for ABA synthesis (for example *sitiens* and *flacca* in tomato, and *droopy* in potato) are not able to close their stomata, though the lesion can be reverted by the supply of exogenous ABA (see e.g. Addicott 1983). Although there are several reports (e.g. Henson 1981) that endogenous ABA concentrations do not always correlate well with stomatal aperture, particularly during recovery from stress, it is possible that these observations may be explained in terms of compartmentation into physiologically active and inactive pools, or that other compounds are involved. The inhibition of stomatal opening by ABA requires the presence of calcium ions; this observation, taken together with evidence that two groups of compounds (calcium channel blockers and calmodulin antagonists) that are known to interfere with the action of calcium as a 'second messenger', also reduce the ability of stomata response to ABA, suggests that calcium may be involved in stomatal responses to ABA (de Silva *et al.* 1985; Davies & Jones 1991).

Methods of study

The stomatal pathway and the corresponding resistance (r_s) or conductance (g_s) to mass transfer is only one component of the total leaf resistance (r_ℓ) (Fig. 6.3). The cuticular transfer pathway (r_c) is in parallel with the stomata, while there is also a transfer resistance within the intercellular spaces (r_i) and, in series with that, a possible wall resistance (r_w) at the surface of the mesophyll cells. Many methods for determining r_s include these other resistances so more correctly provide a measure of r_ℓ; furthermore they often include a boundary layer component. Throughout this book r_ℓ will be used as a measure of r_s, even though these terms are not exactly equivalent. The relative values of stomatal and other components of r_ℓ are discussed in detail below. It follows from discussion in Chapter 3 that stomatal resistances for different gases are inversely proportional to their diffusion coefficients.

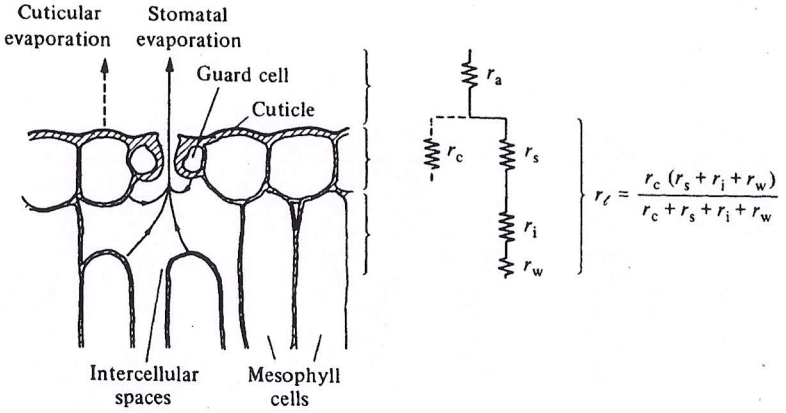

Fig. 6.3. Pathways for water loss from one surface of a leaf, showing the boundary layer (r_a), cuticular (r_c), stomatal (r_s), intercellular space (r_i), wall (r_w), and leaf (r_ℓ) resistances. The total leaf resistance is the parallel sum of r_ℓ for upper and lower surfaces.

Although the most physiologically meaningful measure of stomatal functioning is the diffusion resistance (or conductance), techniques that measure other parameters are widely used (Weyers & Meidner 1990). Important techniques include the following.

Microscopic measurement

Anatomical measurements *in vivo*, as well as on fixed and cleared leaves or epidermal imprints, allow one to quantify the size of the stomatal complexes and their frequency on leaf surfaces. Much of our current knowledge of stomatal physiology derives from studies using isolated epidermal strips where changes in pore size can be followed microscopically. A convenient method for obtaining epidermal imprints is to spread a solution such as nail varnish over the epidermis, allow it to dry, peel it off and store in small envelopes for subsequent microscopic examination. Although useful for counting stomata and for measuring their dimensions, it is difficult to determine apertures from imprints as the impression material may not rupture at the narrowest part of the pore. It is always necessary to demonstrate that microscopic measurements, whether on living or prepared material, isolated epidermes or replicas, are representative of the situation *in vivo*, though it has been suggested that accurate measurements can be obtained using low-temperature scanning electron microscopy where ultra-rapid cryofixation can avoid aperture changes (van Gardingen *et al.* 1989).

Anatomical measurements may be used to derive estimates of the stomatal diffusion resistance (r_s) using diffusion theory (see e.g. Penman & Schofield 1951). For the simplest case of a cylinder or other shape of constant cross-section, the resistance of the pore (s m^{-1}) is given by equation 3.21 as

$$r_s = \ell/\boldsymbol{D} \tag{6.1}$$

where ℓ is the length of the tube and $\boldsymbol{D}$ is the diffusion coefficient.

This resistance per unit pore area can be converted to a resistance per unit area of leaf by dividing by the ratio of average pore cross-sectional area to leaf surface area. For circular pores this ratio in $v\pi r^2$, where v is the frequency of stomata per unit leaf area and r is the pore radius. This gives the stomatal resistance on a leaf area basis as

$$r_s = \ell/v\pi r^2\boldsymbol{D} \tag{6.2}$$

Because the pore area is much less than the leaf area there is a zone close to the pore where the lines of flux converge on the pore. Therefore this zone of the boundary layer is not effectively utilised for diffusion and there is an extra resistance or 'end-effect' associated with each pore. The magnitude of this extra resistance can be derived from three-dimensional diffusion theory as being proportional to pore radius and equal to $\pi r/4\boldsymbol{D}$. Therefore converting to a leaf area basis and adding this extra resistance to the pore resistance gives

$$r_s = [\ell + (\pi r/4)]/v\pi r^2\boldsymbol{D} \tag{6.3}$$

This approach can be extended to other shaped pores and to the estimation of the small intercellular space resistance (Fig. 6.3). It is also possible to correct for alterations in $\boldsymbol{D}$ that occur when the pore size is small, and for interactions with other diffusing species (see Jarman 1974), but these effects are small and usually neglected.

Equations 6.1–6.3 can readily be converted to obtain molar resistances if we remember that the molar resistance ($r^m = r$) can be obtained from r by multiplying by ($\mathscr{R}T/P$) (see equation 3.23*b*).

Infiltration

Graded solutions of differing viscosity (e.g. various mixtures of liquid paraffin and kerosene) have been widely used to estimate relative stomatal opening (see Hack 1974). The viscosity of the solution that just infiltrates the pores provides a measure of aperture. Because of differences in anatomy of pores in different species and differences in cuticular composition, this

approach is only of use for studying qualitative differences within one species.

Viscous-flow porometers

The mass flow of air through stomata under a pressure gradient has been widely used as a measure of stomatal aperture since the first viscous-flow 'porometer' was constructed by Darwin & Pertz in 1911. Air may be forced through the stomata in either of the ways illustrated in Fig. 6.4 and the viscous-flow resistance derived from the measured flow rate or the rate of pressure change (see Meidner & Mansfield 1968). The mass flow rate is inversely proportional to the viscous-flow resistance. This resistance in turn depends on the apertures of the stomata, which constitute the major resistance, and to a lesser extent on resistance to mass flow through the intercellular spaces in the leaf mesophyll (see Fig. 6.4).

Unfortunately there are difficulties in absolute calibration because of the complexity of the flow paths. Furthermore the resistance obtained with trans-leaf flow porometers (Fig. 6.4*a*) is the *sum* of the resistances of the upper and lower surfaces, since they are in series, and is dominated by the larger (usually that of the upper epidermis). However, for diffusive exchange of CO_2 or water vapour, the upper and lower pathways are in parallel, so that the diffusive resistance is largely dependent on the smaller of the two resistances (usually the lower epidermis). Results obtained with viscous-flow porometers must, therefore, be interpreted with care. Nevertheless viscous-flow porometers are particularly useful for continuous recording (a typical example is illustrated in Fig. 6.4*c*). Theoretical and experimental results indicate that diffusive resistances are proportional to the square root of the viscous-flow resistance.

Diffusion porometers

These instruments measure diffusive transfer and are therefore the most relevant and useful for studies of leaf gas exchange. The several trans-leaf diffusion porometers that measure diffusion of gases such as hydrogen, argon or nitrous oxide (see Meidner & Mansfield 1968) are, however, subject to many of the criticisms of the trans-leaf viscous-flow porometers and are little used nowadays. Currently the designs of most of the widely used instruments are based on the measurement of the rate of diffusive water loss from plant leaves. As such they all measure the leaf resistance to water vapour (including any cuticular component) together with any boundary layer resistance in the porometer chamber.

The leaf resistance may be obtained for any sample by subtracting the

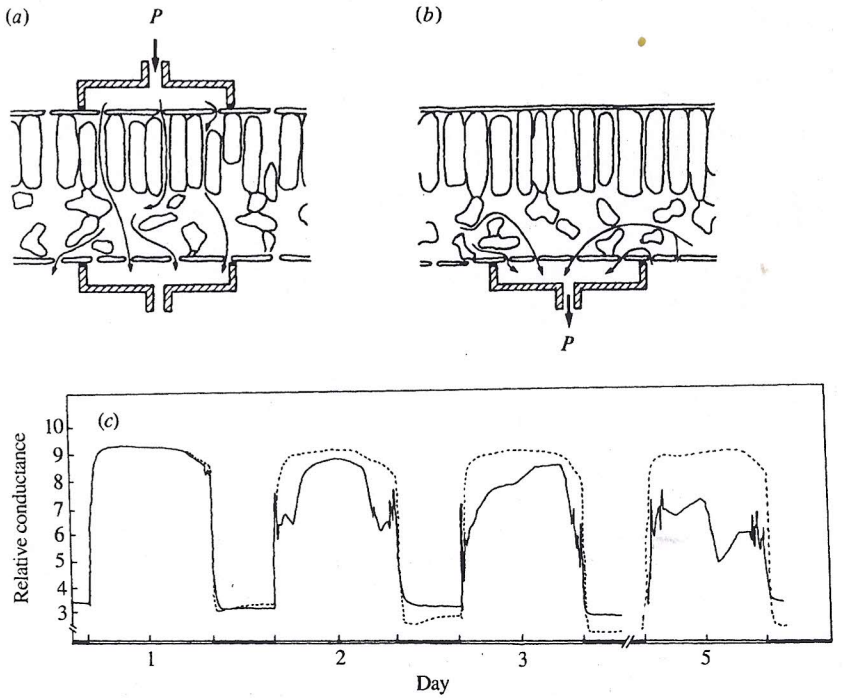

Fig. 6.4. Mass-flow (or viscous-flow) porometers: (*a*) trans-leaf type, (*b*) one-cup type. The applied pressure (*P*) may be above or below atmospheric, and either the flow rate or the rate of change of *P* measured. (*c*) Typical viscous-flow porometer traces for a control leaf of *Helianthus* (dashed line) and for a corresponding leaf on a plant whose roots had been placed in moist air near the start of day 1 (solid line) (data from Neales *et al.* 1989).

chamber boundary layer resistance (a chamber constant usually determined by using water-saturated blotting paper in place of the leaf as described in Appendix 8) from the total resistance observed. The value of this chamber boundary layer resistance may be minimised by stirring the air in the chamber with a small fan.

(i) *Transit-time instruments.* The principle of this type of instrument is that when a leaf is enclosed in a sealed chamber, evaporation will tend to increase the humidity in the chamber at a rate dependent, among other things, on the stomatal diffusion resistance. The time taken for the humidity to increase over a fixed interval can be converted to resistance by the use of a previously obtained calibration curve. Calibration involves replacing the leaf by a wet surface (e.g. wet blotting paper) covered with a calibration plate or microporous membrane (e.g. Celgard 2400) that has a known

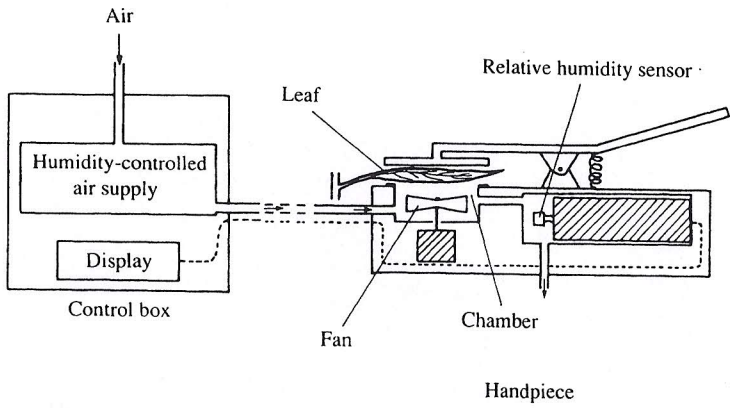

Fig. 6.5. Flow diagram of a typical continuous-flow porometer.

diffusion resistance. Calibration plates with a range of resistances are obtained by varying the number and size of precision drilled holes, with the resistance for any plate being obtained from theory (equation 6.3).

There are several designs of transit-time porometer, many of which are available commercially. Different instruments may include stirring in the chamber to minimise the chamber boundary layer resistance and may be used on irregular leaves or even conifer needles, while others include automatic timing, automatic purging of the chamber with dry air between measurements, or the facility for changing the humidity range over which they operate so as to mimic natural conditions as closely as possible, together with microprocessors to calculate and store data as necessary. In practice the main source of error occurs when leaf temperature (T_ℓ) is not the same as the cup temperature. In such cases porometer estimates of g_ℓ may underestimate the real differences between droughted and well-watered plants (Meyer *et al.* 1985).

(ii) *Continuous-flow (= steady-state) porometers.* The principle of this equipment has long been used in laboratory gas exchange equipment and in recent years has been adapted to field instruments (Fig. 6.5). When a leaf is enclosed in a chamber through which air is flowing, the evaporation rate into the cuvette (in molar units) can be calculated approximately from the product of the flow entering the chamber and the concentration differential across the chamber as

$$\mathrm{E^m} = u_\mathrm{e}(e_\mathrm{o}-e_\mathrm{e})/(PA) = u_\mathrm{e}(x_\mathrm{wo}-x_\mathrm{we})/A \qquad (6.4)$$

where $\mathrm{E^m}$ is the evaporation rate (mol $\mathrm{m^{-2}\,s^{-1}}$), u is the molar flow rate (mol $\mathrm{s^{-1}}$), x_w is the mole fraction of water vapour (mol $\mathrm{mol^{-1}}$), A is the leaf surface area ($\mathrm{m^2}$) exposed in the chamber, and the subscripts 'o' and 'e' refer to the outlet and inlet flows respectively. This equation is only approximate because the water transpired by the leaf changes the flow rate across the cuvette, so it is better to use the full mass balance

$$\mathrm{E^m} = (u_\mathrm{o}x_\mathrm{wo}-u_\mathrm{e}x_\mathrm{we})/A \qquad (6.5)$$

The difference between u_o and u_e equals the evaporation rate (the CO_2 exchange by the leaf may be ignored because it is comparatively small and is largely balanced by O_2 exchange) so that one can write

$$u_\mathrm{o} = u_\mathrm{e}+(u_\mathrm{o}x_\mathrm{wo}-u_\mathrm{e}x_\mathrm{we}) \qquad (6.6a)$$

which rearranges to

$$u_\mathrm{o} = u_\mathrm{e}\frac{(1-x_\mathrm{we})}{(1-x_\mathrm{wo})} \qquad (6.6b)$$

which on substituting back into equation 6.5 gives

$$\mathrm{E^m} = \frac{u_\mathrm{e}(x_\mathrm{wo}-x_\mathrm{we})}{A(1-x_\mathrm{wo})} \qquad (6.7)$$

The term $(1-x_\mathrm{wo})$ in the denominator of equation 6.7 adjusts the flow rate for the amount added by the transpiration from the leaf, though for typical conditions this leads to a correction of only 2–4%. Equivalent equations can be written for E (expressed as a mass flux density) using volume flow rates and concentrations (see Chapter 3).

The evaporation rate is related to the total resistance to water vapour loss $(r_{\ell\mathrm{w}}+r_\mathrm{aw})$, where r_aw is the chamber boundary layer resistance, by

$$\mathrm{E^m} = \frac{(x_{\mathrm{w}s}-x_\mathrm{wo})}{(r_{\ell\mathrm{w}}+r_\mathrm{aw})} \qquad (6.8)$$

where the water vapour pressure at the evaporating sites within the leaf is assumed equal to the saturation vapour pressure at leaf temperature ($e_{s(T\ell)}$) and $x_{\mathrm{w}s}$ is the corresponding mole fraction, and x_wo is assumed to be representative of the mole fraction of water vapour in the chamber air.

Eliminating $\mathrm{E^m}$ from equations 6.7 and 6.8 leads to

$$(r_{\ell\mathrm{w}}+r_\mathrm{aw}) = g_\mathrm{w}^{-1} = \frac{A(x_{\mathrm{w}s}-x_\mathrm{wo})(1-x_\mathrm{wo})}{u_\mathrm{e}(x_\mathrm{wo}-x_\mathrm{we})} \qquad (6.9)$$

Application of this equation can be greatly simplified if air temperature equals leaf temperature (i.e. the system is isothermal) and if dry air is input to the chamber (i.e. $x_\mathrm{we}=0$). Making the approximation that the term $(1-x_\mathrm{wo}) \simeq 1$, this equation simplifies to

$$r_{\ell\mathrm{w}} = 1/g_{\ell\mathrm{w}} = \{[(1/h)-1]\,A/u_\mathrm{e}\}-r_\mathrm{aw} \qquad (6.10)$$

where h is the relative humidity of the outlet air $(= x_\mathrm{wo}/x_{\mathrm{w}s})$.

Unfortunately equations 6.9 and 6.10, though adequate for many purposes, do not take account of the fact that the total transpiration from the leaf is made up of a diffusive component given by equation 6.8 and an additional mass flow equal to the mean water vapour mole fraction along the diffusion pathway from the intercellular spaces times the evaporation rate. Adding this correction to equation 6.8 gives (von Caemmerer & Farquhar 1981)

$$E^m = \left\{\frac{x_{ws}-x_{wo}}{r_{\ell w}+r_{aw}}\right\} + E^m\left\{\frac{x_{ws}+x_{wo}}{2}\right\} \qquad (6.11)$$

Rearranging equation 6.11, and substituting from equation 6.7 gives the following complete expression for the total resistance or conductance to water vapour

$$g_w = (r_{\ell w}+r_{aw})^{-1} = \frac{u_e(x_{wo}-x_{we})\{1-(x_{ws}+x_{wo})/2\}}{A(1-x_{wo})(x_{ws}-x_{wo})} \qquad (6.12)$$

The correction involved is normally of the order of 2–4%, so is only important for accurate work, especially where one is attempting to calculate an intercellular space CO_2 concentration (see Chapter 7).

Estimation of leaf temperature in porometers. Accurate estimation of g_ℓ is dependent on precise estimation of T_ℓ. Although it is common practice to estimate T_ℓ in leaf chambers and porometers by means of thermocouples appressed to the leaf surface, these tend to lead to an estimate of T_ℓ intermediate between the true value and T_a, with consequent errors in g_ℓ. An alternative approach is to estimate the leaf–air temperature difference by means of the leaf energy balance (Parkinson & Day 1980).

Figure 6.5 shows a typical flow diagram of a continuous-flow porometer. These instruments may be used with a constant flow rate (e.g. Parkinson & Legg 1972; Day 1977), in which case the relative humidity of the outlet air is uniquely related to r_ℓ (irrespective of temperature). Alternatively the instruments may be operated in a null-balance mode where the flow rate is adjusted to give a particular relative humidity (see Beardsell *et al.* 1972). Because of stomatal sensitivity to ambient humidity (see below), it is preferable to operate with the chamber humidity close to ambient, whichever mode of operation is used.

Continuous-flow porometers provide the best method currently available for rapid but accurate studies of stomatal conductance in the field. They can vary in sophistication from simple instruments having only an air supply, a leaf chamber and a humidity sensor (Fig. 6.5) to instruments that include temperature measurement and control and readout in conductance units. One advantage over transit-time instruments is that calibration only involves calibration of the humidity sensor and flow meter and one does not need to take account of actual temperature (though see Parkinson & Day 1980) so long as a relative humidity sensor is used. Equally important is the fact that continuous-flow porometers have similar sensitivity over a wide range of g_ℓ. This is in contrast to transit-time instruments that are relatively insensitive at the physiologically important high values of g_ℓ.

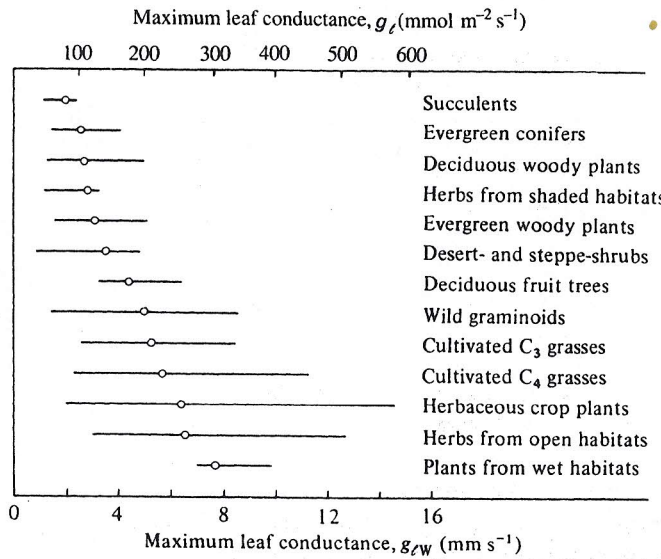

Fig. 6.6. Maximum leaf conductance ($g_{\ell w}$) in different groups of plants. The lines cover about 90% of individual values reported. The open circles represent group average conductances. (Adapted from Körner *et al.* 1979).

Stomatal response to environment

Maximum conductance

The great variability in stomatal frequency and size that exists between different species, leaf position or growth condition (Table 6.1) leads us to expect corresponding differences in stomatal conductance. Figure 6.6 summarises a large number of reported measurements of maximum leaf conductance that have been reported for different groups of plants. Although the range of values found within any group is very wide, there are some clear-cut differences with maximum conductances ($g_{\ell w}$ on a total leaf surface area basis) averaging less than 80 mmol m^{-2} s^{-1} (2 mm s^{-1}) for succulents and evergreen conifers and four times that value for plants from wet habitats.

In addition to genotypic differences, maximum leaf conductance is strongly affected by growth conditions and changes with leaf age.

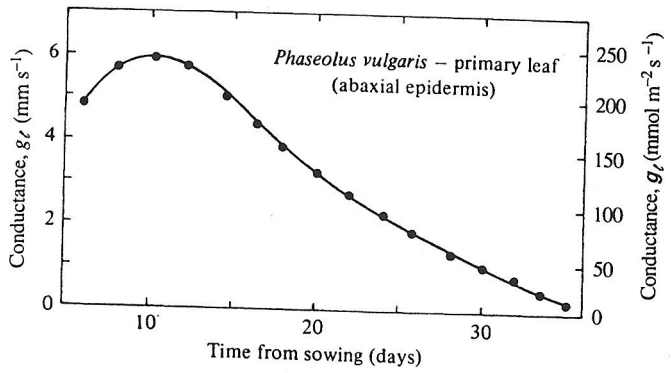

Fig. 6.7. Typical trend of leaf conductance (at 1200 μmol m^{-2} s^{-1}) for a single leaf from early expansion to final senescence. (After Solárová 1980.)

Characteristically, maximum conductance does not attain a peak value until several days after leaf emergence, it may then stay close to this value for a time that is characteristic of the species, finally declining to a very low value as the leaf senesces (Fig. 6.7).

Stomatal response to environment

The effects of individual factors such as radiation, temperature, humidity or leaf water status on stomatal conductance can be studied best in controlled environments or leaf chambers where each factor may be varied independently. However, the use of this information to predict the stomatal conductance in a natural environment is complicated by various factors including (i) interactions between the responses (that is any response depends on the level of other factors), (ii) variability of the natural environment, (iii) the fact that the stomatal time response is frequently of the same order or longer than that of changes in the environment (therefore stomata rarely reach the appropriate steady-state aperture), (iv) in species with amphistomatous leaves the stomata on the upper surface tend to be more responsive than those on the lower surface, and (v) endogenous rhythms tend to affect stomatal aperture independently of the current environment (e.g. night-time closure tends to occur even in continuous light).

Environmental factors affecting stomatal aperture include the following:

(*a*) *Light*. Perhaps the most consistent and well-documented stomatal response is the opening that occurs in most species as irradiance increases (Fig. 6.8*a*). Maximum aperture is usually achieved with irradiances greater than about a quarter of full summer sun (i.e. about 200 W m^{-2} (total

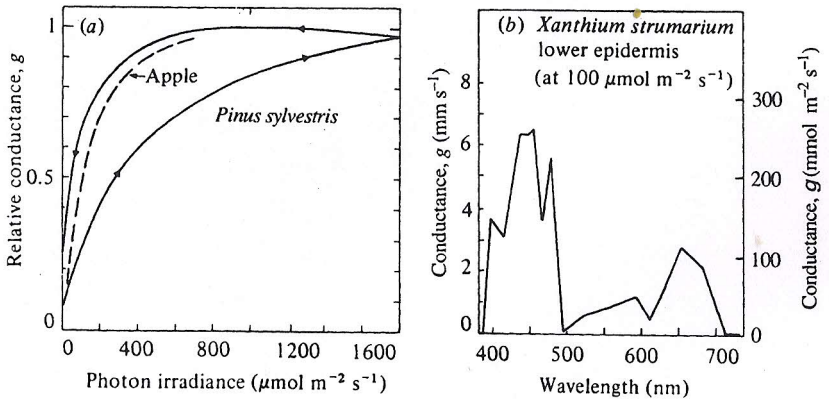

Fig. 6.8. (*a*) Examples of stomatal light response curves. The curve for apple (data from Warrit *et al.* 1980) is typical for many species, approaching a maximum at about a quarter full sunlight. The curves for *Pinus sylvestris* (after Ng & Jarvis 1980) illustrate the hysteresis that can occur in certain conditions. (*b*) Action spectrum of stomatal opening in *Xanthium strumarium* (calculated from Sharkey & Raschke 1981). Action is represented as the conductance achieved at each wavelength for a photon irradiance of 100 μmol m^{-2} s^{-1}.

shortwave) or 400 μmol m^{-2} s^{-1} (PAR)), though this value depends on species and on the natural radiation environment: stomata on shade-grown leaves open at lower light levels than do those on sun-adapted leaves. The conductance–irradiance relationship often shows hysteresis (Fig. 6.8*a*), particularly if time is not allowed for complete equilibrium when the light is altered. Although some of the stomatal response to light may be indirect and attributable to the decrease in intercellular CO_2 concentration that occurs on illumination (see below), there is strong evidence for a direct light response involving two independent photoreceptors. Stomata are particularly sensitive to blue light (Fig. 6.8*b*), a response that probably involves a flavin photoreceptor. The rather smaller response to red light is important at high irradiances and probably involves chlorophyll. Evidence for this comes from the observation that sensitivity to blue light but not to red is found in the white part of variegated leaves.

The rate of stomatal response to changing light is variable, though closing responses tend to be more rapid than opening. Half-times are generally of the order of 2–5 min, which are of the same order as environmental changes. There is some evidence that stomatal closure in response to decreasing light can be potentiated by water stress. An example is shown for sorghum leaves in Fig. 6.9 where mild water deficits decreased the half-time for closure to less than 1 min. The kinetics of response are

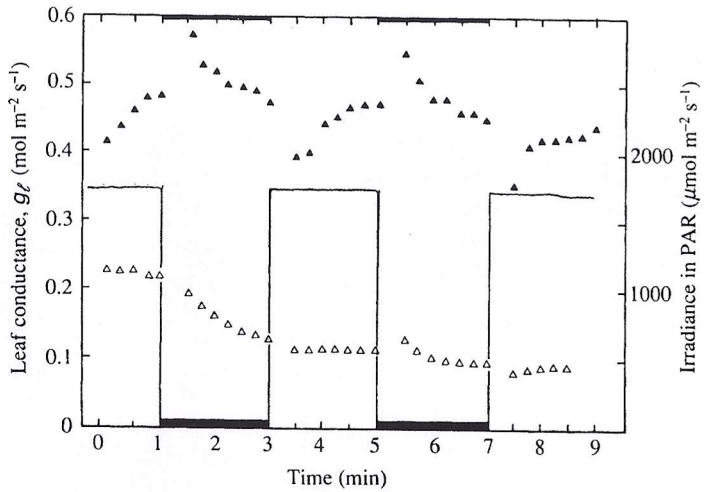

Fig. 6.9. The time course of stomatal conductance for leaves of field-grown *Sorghum bicolor* in response to sudden darkening for well-watered plants (▲) or for plants subject to mild drought (△); irradiance in the PAR is indicated by the continuous line (H. G. Jones, D. O. Hall & J. E. Corlett, unpublished data). The transients obtained on changing irradiance are artefacts related to time for the porometer system to reach equilibrium.

likely to be particularly important when light is changing rapidly, as in sunflecks.

Although in most plants stomata open in response to light and close in the dark, the reverse is true in plants having the Crassulacean acid metabolism (CAM) pathway of photosynthesis (see Chapter 7). In these plants maximal opening is in the dark, particularly in the early part of the night period.

(*b*) *Carbon dioxide.* Although the CO_2 concentration in the natural environment is relatively constant (see Chapter 11), stomata are sensitive to CO_2, responding to the CO_2 mole fraction in the intercellular spaces (x_i'). In general stomata tend to open as x_i' decreases, with the sensitivity to CO_2 being strongly species and environment dependent, being greatest in C_4 species, and at concentrations below about 300 vpm (Morison 1987). Stomata respond to CO_2 in both light and dark, so the response cannot depend only on photosynthesis. The value of x_i' is maintained surprisingly constant (at approximately 130 vpm in C_3 species and 230 vpm in C_4 species), over a wide range of conditions and rates of photosynthesis (Wong *et al.* 1979). This would occur if stomatal conductance varied in proportion to assimilation rate, and has led to the suggestion that a signal from the

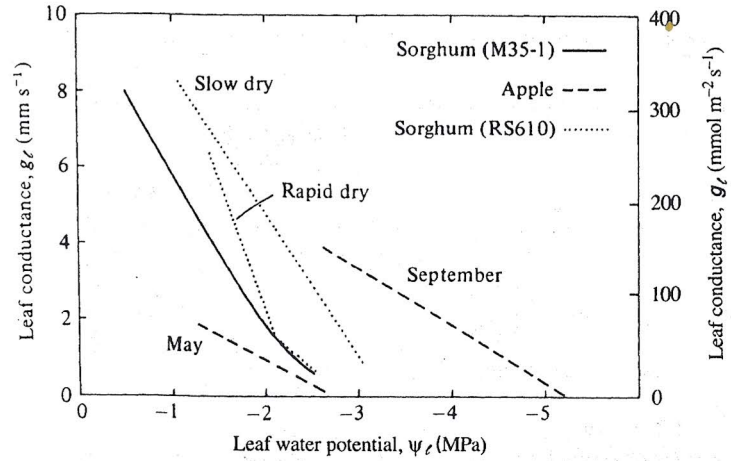

Fig. 6.10. Relationships between g_ℓ and Ψ_ℓ for apple (after Lakso 1979), and sorghum (data from Henzell *et al.* 1976, and Jones & Rawson 1979). Slow drying at 0.15 MPa day^{-1}, fast drying at 1.2 MPa day^{-1}.

mesophyll controls stomatal aperture, though mechanistic evidence for such a hypothesis is lacking and it seems more likely that this results more from a close matching of g_s and assimilation rate.

(*c*) *Water status.* Stomata are sensitive to leaf water status, tending to close with decreasing leaf water potential (Fig. 6.10). Closure occurs over a wide range of Ψ_ℓ, and this relationship can be modified by exposure to previous stress, or by the rate of desiccation. The effects of growth conditions on the Ψ_ℓ at which g_ℓ tends to zero are summarised for several species in Table 6.2. The degree of adjustment ranged from zero for *Hibiscus* to 3.6 MPa for *Heteropogon.* At the leaf water potentials that occur normally for well-watered plants during the course of a day, however, stomatal conductance is relatively insensitive to Ψ_ℓ, and may even *increase* with decreasing leaf water potential (see Fig. 6.14*d* and Jones 1985*b*); this response is what one would expect if stomatal conductance were controlling leaf water potential (through an altered transpiration rate), rather than the reverse and is discussed further below.

Although it is clear from studies with detached leaves that stomata can respond to leaf water status through locally mediated effects on active solute accumulation in the guard cells, there are several lines of evidence that stomatal closure in response to soil drying may often be controlled by other factors (see also Chapter 4). For example, when the leaf water status of *Helianthus annuus* and *Nerium oleander* plants was manipulated by modifying the whole-plant transpiration by changes in atmospheric

Table 6.2. *Some examples of stomatal adaptation to stress in different species*

Species	Condition	Ψ_ℓ at which g_ℓ tends to zero (MPa)			
		Maximum	Minimum	Adjustment	Ref.
Apple	Seasonal change, field	−2.7	−5.2	2.5	1
Heteropogon contortus	CE vs field	−1.4	−5.3	3.6	2
Eucalyptus socialis	Outdoor hardening	−2.5	−3.8	1.3	3
Cotton	CE vs field	−1.6	−2.7	1.1	4
Cotton	Drought cycles in CE	−2.8	−4.0	1.2	5
Sorghum	Field	−1.9	−2.3	0.4	6
Wheat	CE, solution culture	−1.4	−1.9	0.5	7
Hibiscus cannabinus	CE vs field	−2.1	−2.0	0	2

CE refers to controlled environment.
References: 1. Lakso 1979; 2. Ludlow 1980; 3. Collatz *et al.* 1976; 4. Jordan & Ritchie 1971; 5. Brown *et al.* 1976; 6. Turner *et al.* 1978; 7. Simmelsgaard 1976.

humidity, while maintaining fixed environmental conditions for an individual leaf whose conductance was monitored, it was found that leaf conductance of the monitored leaf was much more closely related to soil water status than to leaf water status (Fig. 6.11). The hypothesis that leaf conductance could respond directly to soil water status was tested further by pressurising the root system to maintain pressure in the xylem at zero (thus maintaining the leaf cells fully turgid), as soil was allowed to dry (Gollan *et al.* 1986). Again leaf conductance appeared to respond to soil water content, rather than to leaf turgor (Fig. 6.12).

Further evidence that soil water status may, on occasions, be more important than the water status of the leaf itself in controlling g_ℓ has been discussed in Chapter 4. It is commonly observed that stomatal conductance is better related to Ψ_p than to Ψ_ℓ, with at least some of the change in response to growth conditions (Table 6.2) being related to osmotic adjustment (see Chapter 10) where a given turgor pressure is achieved at a lower water potential as a result of solute accumulation in the cell sap. It is likely that the close relationship to bulk leaf Ψ_p, where it is observed, is indirect, acting through an effect on ion pumping at the guard cells.

When a plant is re-watered after a period of drought, the stomata may

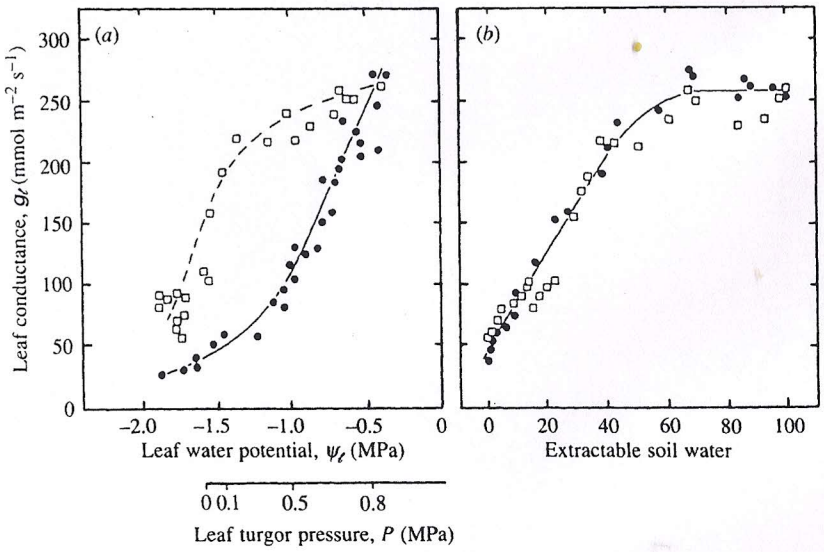

Fig. 6.11. (*a*) Relationship between leaf conductance and Ψ_ℓ in *Nerium oleander* as soil water content decreased and the leaf-to-air vapour concentration difference ($\delta x_{w\ell}$) was maintained at 10 Pa kPa^{-1} while the whole plant was maintained either in an atmosphere with a constant vapour concentration difference of 10 Pa kPa^{-1} (●) or where the concentration difference was as great as 30 Pa kPa^{-1} (□). (*b*) The data from (*a*) replotted as a function of extractable soil water. (Redrawn from Schulze 1986 with data from Gollan *et al.* 1985.)

take some days to recover (depending on the severity and duration of the stress), even though leaf water potential may recover rapidly.

(*d*) *Humidity*. Until the early 1970s it had been thought that stomata were insensitive to ambient humidity. For example Meidner & Mansfield (1968) in their text on stomatal physiology state '... stomatal behaviour ... is comparatively unaffected by changes in relative humidity of the ambient air'. It is now clear, however, that the stomata in many species close in response to increased leaf-to-air vapour pressure difference (δe_ℓ), as shown in Fig. 6.13. The magnitude of this response is dependent on species, growing conditions and particularly plant water status, the response being smaller at high temperature (Fig. 6.13) or in stressed plants.

Although the humidity response frequently takes minutes to reach full expression, it has been reported, at least for apple leaves, that as much as 90% of the total stomatal response to an increased δe_ℓ can occur within 20 s of the change (Fanjul & Jones 1982). Opening responses tend to be rather slower.

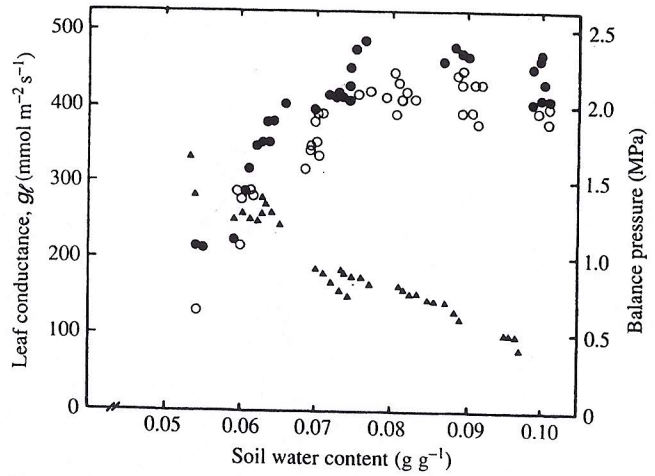

Fig. 6.12. Relationship between leaf conductance (g_ℓ) and soil water content for wheat leaves, when the soil was dried either without maintaining leaf turgor by pressurising the system (○) or with maintenance of leaf turgor by applying a balancing pressure (●). The corresponding values of the balancing pressure (P) required to maintain turgor at each soil water content are indicated by (▲). (Data from Gollan *et al.* 1986.)

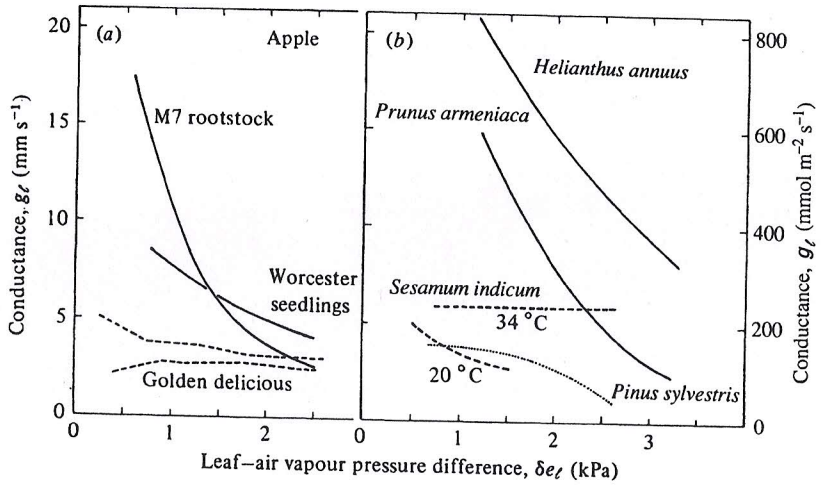

Fig. 6.13. Examples of stomatal humidity responses. (Data for apple from Warrit *et al.* 1980 and Fanjul & Jones 1982; *Helianthus* and *Sesamum* from Hall & Kaufmann 1975; *Prunus* from Schulze *et al.* 1972; and *Pinus* from Jarvis & Morison 1981.)

(*e*) *Temperature.* Many studies of stomatal temperature responses have yielded contradictory results. Unfortunately, in many earlier studies temperature was confounded with variation in leaf–air vapour pressure difference. It is necessary to conduct temperature response studies at constant values of δe_ℓ (under which conditions absolute and relative humidity increase with temperature). In general, stomata tend to open as temperature increases over the normally encountered range, though an optimum is sometimes reached (see Hall *et al.* 1976). The magnitude of the temperature response does, however, depend on the vapour pressure.

(*f*) *Other factors.* Stomatal aperture is also affected by many gaseous pollutants such as O_3, SO_2 and nitrogen oxides (Mansfield 1976; Unsworth & Black 1981). Many of these responses are probably related to the toxic effects of these substances on membrane integrity. Stomatal aperture is also dependent on many other factors such as leaf age, nutrition and disease.

Stomatal behaviour in natural environments

As pointed out earlier, it is difficult to determine stomatal responses from measurements in the field. Typical results for leaf conductance of extension leaves of apple trees during the course of one day are presented in Fig. 6.14, together with the irradiance on a horizontal surface. These results are also plotted against irradiance and Ψ_ℓ in Fig. 6.14*b* and *d*. The variability in g_ℓ is a result partly of the fluctuations in irradiance and partly of leaf-to-leaf variability and differences in orientation. Much of the scatter in the plot of g_ℓ against **I** (Fig. 6.14*b*) results from the stomatal time constant being longer than that of the fluctuations of irradiance.

Several approaches can be used to determine the stomatal response to individual factors or to predict g_ℓ for given conditions, using results such as those in Fig. 6.14. One approach is to use boundary-line analysis. In Fig. 6.14*b* a hypothetical ideal boundary-line relationship between g_ℓ and **I** is shown as the dashed line, which may approximate the response when no other factors are limiting. It is assumed that many points fall below this line as a result of factors such as lowered Ψ_ℓ. Unfortunately this approach is difficult to quantify statistically as the upper points that define the boundary line are measured with some degree of error.

A widely used approach is that of multiple regression, where g_ℓ is regressed against various independent variables to give an equation of the form

$$g_\ell = a + b\mathbf{I} + c\delta e_\ell + d\Psi_\ell + \ldots \qquad (6.13)$$

where a, b, c, d, etc. are regression coefficients. Non-significant terms can

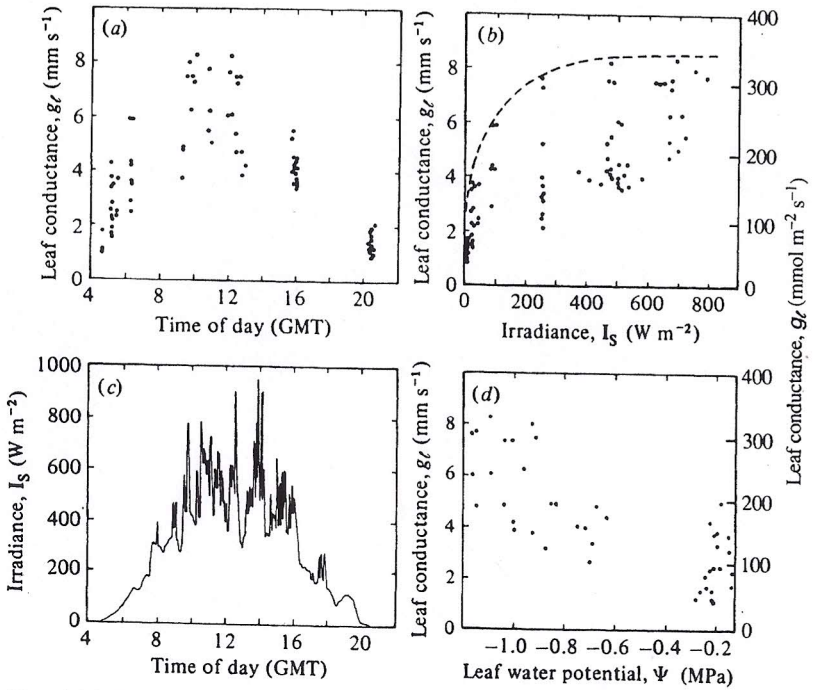

Fig. 6.14. Typical variation during one day (26 July 1980) of g_ℓ of mid-extension leaves of Bramley apples (*a*), together with irradiance above the canopy (*c*), and g_ℓ as a function of I (*b*) or Ψ_ℓ (*d*). For details see text. (H. G. Jones, unpublished data.)

be omitted and non-linear relations fitted by the use of higher-order polynomials (e.g. quadratic). This technique can give useful summaries of large amounts of data, but it is entirely empirical and thus has rather little predictive value for untried combinations of environmental conditions. It is frequently necessary to include time of day as an independent variate.

It is worth noting that the 'important' variates found in multiple regression models are often not the same as the individual variates most closely related to g_ℓ when regressed singly. For example, in an analysis of several data sets for apple in England, Jones & Higgs (1989) showed that the most useful three variates in a multiple regression were δe_ℓ, I_{50} (a derived variate $= I/(50+I)$), and T_a, even though the best individual variates were either *e*, or *h*. This latter observation is of particular interest in relation to the recent suggestion that g_ℓ tends to vary directly in proportion to assimilation rate scaled by the relative humidity at the leaf surface (Ball *et al.* 1986).

In order to get a robust model for predicting g_ℓ Jones & Higgs (1989) proposed the replacement of the environmental variates in equation 6.13 by differences (Δ) from typical values so that equation 6.13 becomes

$$g_\ell = g_o + \beta 1\,\Delta I + \beta 2\,\Delta\delta e + \beta 3\,\Delta\Psi_\ell + \ldots \qquad (6.14)$$

where g_o is a reference value (at typical environmental conditions) and the βi are multiple regression coefficients. For prediction of g_ℓ for new data sets, the sizes of the coefficients can be normalised by dividing through by g_o to give

$$g_\ell = g_o(1 + b1\,\Delta I + b2\,\Delta\delta e + b3\,\Delta\Psi_\ell + \ldots) \qquad (6.15)$$

where the bi $= \beta i/g_o$. The model is scaled to different data sets by using an appropriate g_o; absolute errors in predicted g_ℓ that result from incorrect regression coefficients are minimised by this technique. Using this approach it was shown that a model derived for one data set could fit data sets obtained for other orchards in different years as successfully as a freely-fitted model. The model using δe_ℓ, T_a and I_{50} explained between 32 and 62 % of the variance in g_ℓ for different sets of apple data (Jones & Higgs 1989).

Perhaps the best method for analysing stomatal conductance (see Jarvis 1976) is to use a multiplicative model (rather than the additive model in equation 6.13) with appropriate non-linear components of the form

$$g_\ell = g_o \cdot f(I) \cdot g(\delta e_\ell) \cdot h(\Psi_\ell) \cdot \ldots \qquad (6.14)$$

where the forms of the individual functions (f(I), g(δe_ℓ), etc.) are obtained from controlled environment studies. Some particularly useful functions are summarised in Fig. 6.15. It is worth noting that for well-watered plants the stomata do not usually close in response to the normal diurnal fall in Ψ_ℓ. In fact an opposite effect is sometimes observed (Fig. 6.14*d*). This somewhat paradoxical result (compare with Fig. 6.10) arises because Ψ_ℓ is falling as a result of the increased evaporation rate as stomata open, rather than control operating the other way around.

Stomatal resistance in relation to other resistances

Typical values for the components of leaf and boundary layer resistances to water vapour loss from single leaves (see Fig. 6.3) are summarised in Table 6.3. Although the cuticular resistance tends to be by far the largest, the dominant component of the total resistance is stomatal, because the resistance of two parallel resistors is determined primarily by the smaller.

The high cuticular resistance results from the low water permeability (liquid and vapour) of the hydrophobic cuticle and the overlying wax layer. The thickness, composition and morphology of the cuticle and wax layers

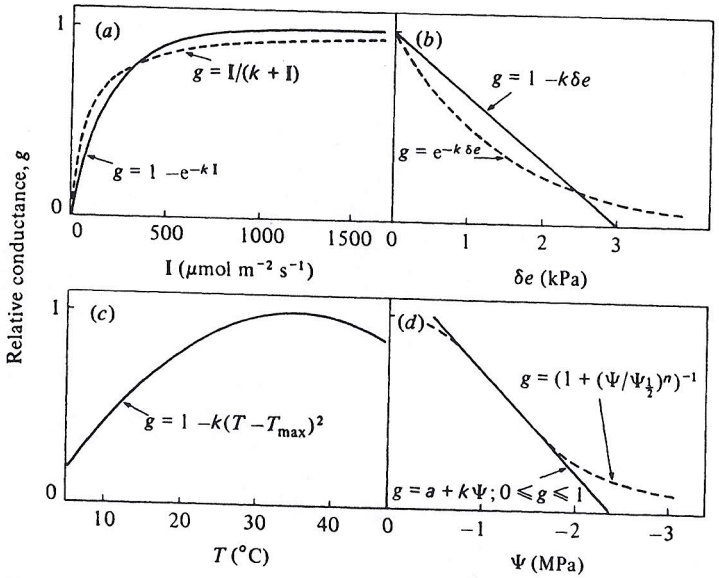

Fig. 6.15. (*a*)–(*d*) The most useful functions for describing stomatal response to environment (solid lines), and other useful functions (dashed lines). *a*, *k*, *n* are constants, as are T_{max} (T at which g is maximal) and $\Psi_{\frac{1}{2}}$ (the value of Ψ when g is half maximum). All functions give g as a fraction of a reference value. Details of the Ψ functions are discussed by Fisher *et al.* (1981).

is very dependent on species and growth conditions (see Martin & Juniper 1970), being most developed (with highest r_c) in plants from arid sites where water conservation is most crucial. The waxes may vary in form from smooth layers or platelets to rods or filaments several micrometres long. Some epidermal wax structures are shown in Fig. 6.2*e*.

Mathematical and physical models of gas diffusion in the intercellular spaces suggest that most transpired water originates from cell walls close to the stomatal pore, so that r_{iw} is small (probably less than 0.5 m² s mol⁻¹) (see Tyree & Yianoulis 1980). Because the sites of CO_2 assimilation are more evenly distributed throughout the leaf, r_{ic} may be significant and perhaps as much as 2.5 m² s mol⁻¹.

There has been controversy about the magnitude of the 'wall' resistance, r_w, since Livingston & Brown (1912) reported evidence for non-stomatal control of water loss. They envisaged that the evaporation sites retreated into the cell walls thus increasing the gas-phase diffusion path, a process they called 'incipient drying'. An alternative possibility is that the effective water vapour concentration at the liquid–air interface is significantly below saturation at leaf temperature. From equation 5.11, the relative lowering of

Table 6.3. *Relative values of the different resistances (see Fig. 6.3) and the corresponding conductances for single leaves. The leaf resistance is dominated by the stomatal component*

		Resistance r^m (m² s mol⁻¹)	Conductance g^m (mmol m⁻² s⁻¹)	Corresponding conductance g (mm s⁻¹)
Intercellular space and wall resistance	($r_i + r_w$)	< 1	> 1000	> 25
Cuticular resistance	(r_c)	50– > 250	4–20	< 0.1–0.5
Stomatal resistance	(r_s)			
– minimum for many succulents, xerophytes and conifers		5–25	40–200	1–5
– minimum for mesophytes		2–6	170–500	4–13
– maximum when closed		> 125	8	< 0.2
Boundary layer resistance	(r_a)	0.25–2.5	400–4000	10–100

the partial pressure of water vapour (e) compared with that at saturation (e_s) is related to water potential by

$$e/e_s = \exp(\Psi \bar{V}_w/\mathscr{R}T) \qquad (6.15)$$

Application of this equation predicts that at 20 °C, e/e_s would be 0.99 at −1.36 MPa, and only falls to 0.95 at −6.92 MPa, a figure found only in extremely severely stressed leaves. For a relative humidity of 0.50 in the ambient air, even this latter figure would introduce less than a 10% error in the driving force for evaporation (or equivalently r_w would be less than 10% of the total resistance).

In addition to effects of bulk leaf water potential on Ψ at the evaporating surface, Ψ could also be lowered by accumulation of solutes, or because of the presence of a large internal hydraulic resistance. Experimental results for several species and theoretical calculations (Jarvis & Slatyer 1970; Jones & Higgs 1980) all suggest that r_w is small ($\ll$ 1 m² s mol⁻¹) at physiological water contents.

Table 6.3 shows that, for single leaves, r_ℓ is normally at least an order of magnitude greater than r_a. In canopies, however, the relative importance of

Table 6.4. *Canopy leaf or physiological resistance to water vapour (r_L) and canopy boundary layer (r_A) resistance for different types of vegetation (from Jarvis 1981). Approximate equivalents in molar units (m^2 s mol^{-1}) are given in parentheses*

	r_L(s m^{-1}) per unit leaf area	r_L (s m^{-1}) per unit ground area	r_A (s m^{-1}) per unit ground area
Grassland/heathland	100 (2.5)	50 (1.25)	50–200 (1.25–5)
Agricultural crops	50 (1.25)	20 (0.5)	20–50 (0.5–1.25)
Plantation forest	167 (4.2)	50 (1.25)	3–10 (0.08–0.25)

the boundary layer resistance increases. This is because all the individual leaf resistances are in parallel and therefore the total leaf resistance decreases as leaf area index increases. In addition, for a crop, the boundary layers for the individual leaves must be added to an overall crop boundary layer. Some typical ranges for the values of the canopy boundary layer resistance (r_A) and the canopy leaf resistance (r_L) are given in mass units (because these are more commonly used for canopy studies) in Table 6.4 (the equivalents in molar units are given in parentheses). The values shown indicate that the ratio between r_A and r_L can vary widely between different plant communities. Some implications of differences in this ratio between grassland and aerodynamically rough canopies such as tall forests, were discussed in Chapter 5.

Stomatal function and the control loops

The two main control systems involved in the regulation of stomatal aperture are related to the fluxes of water vapour and CO_2 that need to be controlled (Fig. 6.1):

(*a*) *Water control loop.* The main function of stomata is the control of water loss. In general they respond to factors that lower Ψ_ℓ in such a way as to minimise further increases in stress. The responses involve either feedback via leaf water status itself, or else direct feedforward control (Fig. 6.1). The distinction between feedback and feedforward can be illustrated by the possible effects of altered δe_ℓ (see Fig. 6.16).

Negative feedback is illustrated by the control pathway in the lower part of Fig. 6.16. Here a decrease in air humidity (increased δe_ℓ) increases E, since

$$\mathrm{E} = (2.17/T)\, g_\ell\, \delta e_\ell \qquad (6.16)$$

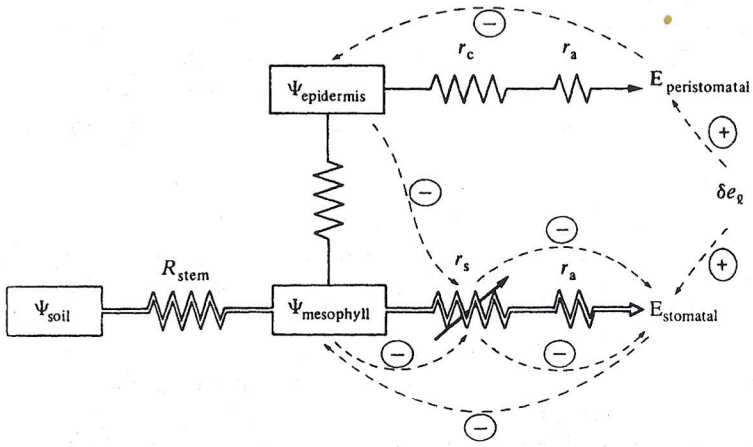

Fig. 6.16. A simplified diagram of the various feedback and feedforward control loops involved in humidity effects on stomatal aperture. The solid lines represent the flows of water with the majority of the flow occurring through (and controlled by) the stomatal pores (double lines) and with only a small proportion of peristomatal evaporation directly through the epidermis (single lines). The dotted lines indicate control processes with the signs indicating the effect of an increase in the first factor on the second (e.g. the negative sign relating $\mathrm{E}_{stomatal}$ to $\Psi_{mesophyll}$ indicates that an increase of $\mathrm{E}_{stomatal}$ results in a decrease of $\Psi_{mesophyll}$).

This in turn tends to lower bulk Ψ_ℓ because, from equation 4.25 (representing the sum of all the soil and plant resistances by R_{sp}):

$$\Psi_\ell = \Psi_s - R_{sp}\,\mathrm{E} \qquad (6.17)$$

This lowered Ψ_ℓ then leads to stomatal closure which finally has a negative feedback effect on E. Assuming a linear relationship (Fig. 6.15*d*):

$$g_\ell = a + b\Psi_\ell \qquad (6.18)$$

and, combining this with equation 6.17 gives

$$g_\ell = a + b(\Psi_s - R_{sp}\,\mathrm{E}) = c - d\mathrm{E} \qquad (6.19)$$

where a, b, c and d are constants. From equations 6.16 and 6.19 the relationships describing this negative feedback are

$$\mathrm{E} = c\delta e_\ell/(1 + d\delta e_\ell) \qquad (6.20)$$

$$g_\ell = c/(1 + d\delta e_\ell) \qquad (6.21)$$

and are illustrated by the solid lines in Fig. 6.17. Note that equation 6.20 is a saturation-type curve and that negative feedback cannot cause a steady-

state reduction in transpiration (dotted curve in Fig. 6.17) as δe_ℓ increases. (Any reduction in E implies increases in Ψ_ℓ and hence g_ℓ which would immediately restore E.) A feedback loop with a high *gain* would tend to maintain E relatively constant. However, a high gain can lead to instability and regular stomatal oscillations (see Cowan 1977) where there are time delays in the responses.

Feedforward is illustrated in the top half of Fig. 6.16. In this case the environment affects the controller (the stomata) directly *without* depending on changes in the flux that is being controlled (i.e. evaporation through the stomata). An increased δe_ℓ increases the rate of peristomatal transpiration (water loss not passing through the stomatal pore). This leads to lowered guard-cell water potential and consequent stomatal closure, as long as the hydraulic flow resistance in the pathway to the evaporating sites on the outer surface of the guard cells is great enough. (Evidence for a significant flow resistance in this pathway is discussed by Meidner & Sheriff (1976).) Using an argument similar to that used to derive equation 6.21, it is possible to show that in this case (cf. Fig. 6.15)

$$g_\ell = e - f\delta e_\ell \tag{6.22}$$

where e and f are constants. Combining with equation 6.16 and rearranging gives

$$\mathrm{E} = e'\delta e_\ell - f'(\delta e_\ell)^2 \tag{6.23}$$

Depending on the relative values of the new constants e' and f', E may even fall with increased evaporative demand (dotted curve in Fig. 6.17). Such responses have been observed in several species. In practice, both feedback and feedforward responses usually occur together. Further discussion of feedback and feedforward in this context may be found in articles by Cowan (1977) and Farquhar (1978). Figure 6.17 also shows the expected linear response of E to δe_ℓ when there is no stomatal response (dashed curve).

The general processes involved in stomatal response to guard cell or mesophyll water status were outlined above, and it was pointed out that although hydropassive movements can occur, and that they may be responsible for the very rapid movements observed on detaching leaves, active responses, probably mediated by ABA, are much the more important.

(*b*) *Carbon dioxide control loop.* The central role of the stomata in the control of photosynthesis depends on sensing the photosynthetic rate. Most evidence indicates that the photosynthetic feedback control (Fig. 6.1) depends on sensing the intercellular space CO_2 concentration. For example, as light increases, the rate of CO_2 fixation increases, thus lowering the intercellular CO_2 concentration, and the stomata open to compensate.

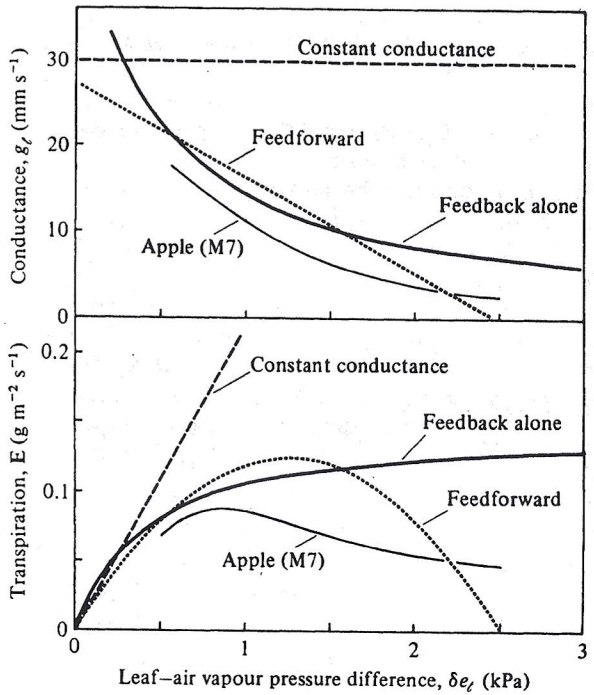

Fig. 6.17. Types of stomatal humidity response and the consequent relation between E and δe_ℓ. The thick solid lines show negative feedback (equations 6.20 and 6.21), the dotted lines show feedforward (equations 6.22 and 6.23) and the dashed line constant g_ℓ. Data for M7 apple from Fig. 6.13 are shown for comparison.

Other changes that reduce the intercellular space CO_2 have a similar effect (though see Jarvis 1980).

There is a strong feedback control that tends to maintain intercellular CO_2 remarkably constant (at a mole fraction of around 130×10^{-6} in C_4 species and 230×10^{-6} in C_3 species – see Chapter 7). The night-time stomatal opening in CAM plants can also be explained on the same basis: dark CO_2 fixation at night lowers intercellular CO_2 and stomata open.

Sample problems

6.1 A leaf detached from a plant and suspended in a moving airstream ($h = 0.2$) initially loses weight at a rate of 80 mg m^{-2} s^{-1}, falling to a constant rate of 2 mg m^{-2} s^{-1} after about 20 min. A piece of wet blotting paper suspended alongside the leaf loses water at a rate of 230 mg m^{-2} s^{-1}. Assuming that leaf, air and blotting paper are all at 20 °C, calculate (i) the boundary layer

resistance, r_{aw}, (ii) the cuticular resistance, r_{cw}, (iii) the initial value of the stomatal resistance, r_{sw}, if the leaf has equal numbers of stomata on each surface.

6.2 Calculate (i) the stomatal diffusion resistance (r_{sw}) and (ii) the corresponding conductance (g_{sw}) for a leaf with 200 stomata mm^{-2} on each surface, each pore being 10 μm deep and circular in cross-section ($d = 5$ μm).

6.3 A continuous-flow porometer with a chamber area of 1.5 cm^2 is attached to the lower surface of a leaf. If the flow rate is 2 $cm^3\ s^{-1}$, and the relative humidity of the outlet air is 35% (inlet air is dry), calculate $g_{\ell w}$ assuming (i) that $T_\ell = T_a$ or (ii) that $T_\ell = 25$ °C and $T_a = 27$ °C.

6.4 Assuming that g_ℓ for a particular species decreases linearly from 10 mm s^{-1} at $\delta e = 0$ kPa to 0 at $\delta e = 3$ kPa: (i) plot a graph of the relationship between **E** and δe; what is **E** when $\delta e = 1$ kPa? (ii) If g_ℓ is also sensitive to Ψ_ℓ, falling by 50% per MPa below zero, plot the dependence of **E** on δe if Ψ_ℓ falls linearly at a rate of 1 MPa for each 0.1 g $m^{-2}\ s^{-1}$ increase in evaporation; what is **E** when $\delta e = 1$ kPa?